



HAL
open science

High-Accuracy Determination of Microsatellite Instability Compatible with Liquid Biopsies

Amanda Bortolini Silveira, François-Clément Bidard, Amélie Kasperek, Samia Melaabi, Marie-Laure Tanguy, Manuel Rodrigues, Guillaume Bataillon, Luc Cabel, Bruno Buecher, Jean-Yves Pierga, et al.

► **To cite this version:**

Amanda Bortolini Silveira, François-Clément Bidard, Amélie Kasperek, Samia Melaabi, Marie-Laure Tanguy, et al. High-Accuracy Determination of Microsatellite Instability Compatible with Liquid Biopsies. *Clinical Chemistry*, 2020, 66 (4), pp.606-613. 10.1093/clinchem/hvaa013. inserm-03034635

HAL Id: inserm-03034635

<https://inserm.hal.science/inserm-03034635>

Submitted on 1 Dec 2020

HAL is a multi-disciplinary open access archive for the deposit and dissemination of scientific research documents, whether they are published or not. The documents may come from teaching and research institutions in France or abroad, or from public or private research centers.

L'archive ouverte pluridisciplinaire **HAL**, est destinée au dépôt et à la diffusion de documents scientifiques de niveau recherche, publiés ou non, émanant des établissements d'enseignement et de recherche français ou étrangers, des laboratoires publics ou privés.

Clinical Chemistry

Manuscript Title: High-accuracy determination of microsatellite instability compatible with liquid biopsies

Manuscript No: CLINCHEM/2019/309807 [R2]

Manuscript Type: Article

Date Submitted by the Author: 23 Dec 2019

Complete List of Authors: Amanda Bortolini Silveira, Francois-Clement Bidard, Amélie Kasperek, Samia Melaabi, Marie-Laure Tanguy, Manuel Rodrigues, Guillaume Bataillon, Luc Cabel, Bruno Buecher, Jean-Yves Pierga, Charlotte Proudhon, and Marc-Henri Stern

Keywords: droplet digital PCR; liquid biopsy; microsatellite instability; mismatch repair deficiency

Dear Reviewer,

Thank you for reviewing this manuscript, please remember the following:

1. The attached manuscript is confidential and should not be circulated or shared with anyone.
2. Authors of this manuscript should never be contacted until after its publication.
3. If you have a conflict of interest regarding this work, contact the editorial office immediately.
4. Be sure to review the authors' potential conflicts of interest by following the "Author Disclosures" link in your reviewer area. Contact the editorial office if you need assistance.

Confidential

1 **High-accuracy determination of microsatellite instability compatible with liquid biopsies**

2 **Running title:** MSI detection in tissue and plasma

3 Amanda Bortolini Silveira¹, François-Clément Bidard^{1,2,3}, Amélie Kasperek¹, Samia

4 Melaabi⁴, Marie-Laure Tanguy⁵, Manuel Rodrigues^{2,6}, Guillaume Bataillon⁴, Luc Cabel^{2,3},

5 Bruno Buecher², Jean-Yves Pierga^{2,7}, Charlotte Proudhon^{1*}, and Marc-Henri Stern^{6*}

6 ¹ Circulating Tumor Biomarkers Laboratory, Institut Curie, PSL Research University,

7 INSERM CIC 1428, Paris, France.

8 ² Department of Medical Oncology, Institut Curie, PSL Research University, Paris, France.

9 ³ Versailles Saint Quentin en Yvelines University, Paris Saclay University, Saint Cloud, Paris,
10 France.

11 ⁴ Department of Biopathology, Institut Curie, PSL Research University, Paris, France.

12 ⁵ Biostatistics unit, Institut Curie, Saint Cloud, Paris, France.

13 ⁶ Inserm U830, DNA Repair and Uveal Melanoma (D.R.U.M.) team, Equipe labellisée par la
14 Ligue Nationale Contre le Cancer, Institut Curie, PSL Research University, Paris, France.

15 ⁷ Paris Descartes University, Paris, France.

16 ***Corresponding authors:**

17 Dr. Charlotte Proudhon, Tel: +33 1 56 24 62 82. Email: charlotte.proudhon@curie.fr

18 Dr. Marc-Henri Stern, Tel: +33 1 56 24 66 46. Email: marc-henri.stern@curie.fr

19 **Keywords:** microsatellite instability, mismatch repair deficiency, droplet digital PCR, liquid
20 biopsy

21

22

23

24 **List of abbreviations:**

- 25 Microsatellite instability (MSI)
- 26 Circulating tumor DNA (ctDNA)
- 27 Droplet digital PCR (ddPCR)
- 28 DNA mismatch repair (MMR)
- 29 Microsatellite stable (MSS)
- 30 Next-generation sequencing (NGS)
- 31 Immunohistochemistry staining (IHC)
- 32 Cell-free DNA (cfDNA)
- 33 Formalin-fixed, Paraffin-embedded (FFPE)
- 34 Limit of detection (LOD)
- 35 Limit of blank (LOB)
- 36 Mutant Allele Frequency (MAF)
- 37 Colorectal cancer (CRC)
- 38 Wild-type (WT)

39

40 **Human genes:**

- 41 *KRAS* (KRAS proto-oncogene, GTPase)
- 42 *BRAF* (B-Raf proto-oncogene, serine/threonine kinase)
- 43 *EGFR* (epidermal growth factor receptor)
- 44 *ACVR2A* (activin A receptor type 2A)
- 45 *DEFB105A/B* (defensin beta 105A/B)
- 46 *PIK3CA* (phosphatidylinositol-4,5-bisphosphate 3-kinase catalytic subunit alpha)
- 47 *MLH1* (mutL homolog 1)
- 48 *MSH2* (mutS homolog 2)

- 49 *MHS6* (mutS homolog6)
- 50 *PMS2* (PMS1 homolog 2)

Confidential

51 **Abstract**

52 Background: Microsatellite instability (MSI) has recently emerged as a predictive pan-tumor
53 biomarker of immunotherapy efficacy, stimulating the development of diagnostic tools
54 compatible with large-scale screening of patients. In this context, non-invasive detection of
55 MSI from circulating tumor DNA stands as a promising diagnostic and post-treatment
56 monitoring tool.

57 Methods: We developed drop-off droplet-digital PCR (ddPCR) assays targeting BAT-26,
58 activin A receptor type 2A (*ACVR2A*) and defensin beta 105A/B (*DEFB105A/B*)
59 microsatellite markers. Performances of the assays were measured on reconstitution
60 experiments of various mutant allelic fractions, on 185 tumor samples with known MSI status,
61 and on 72 blood samples collected from 42 patients with advanced colorectal or endometrial
62 cancers before and/or during therapy.

63 Results: The three ddPCR assays reached analytical sensitivity $<0.1\%$ variant allelic
64 frequency and could reliably detect and quantify MSI in both tumor and body fluid samples.
65 High concordance between MSI status determination by the three-marker ddPCR test and the
66 reference pentaplex method were observed (100% for colorectal tumors and 93% for other
67 tumor types). Moreover, the three assays showed correlations with $r \geq 0.99$ with other
68 circulating tumor DNA markers and their dynamic during treatment correlated well with
69 clinical response.

70 Conclusions: This innovative approach for MSI detection provides a non-invasive, cost-
71 effective and fast diagnostic tool, well suited for large-scale screening of patients that may
72 benefit from immunotherapy agents, as well as for monitoring treatment responses.

73

74 Introduction

75 Tumors with DNA mismatch repair (MMR) deficiency accumulate high numbers of DNA
76 replication errors, particularly deletions at repetitive DNA sequences termed microsatellites.
77 This phenotype, referred to as microsatellite instability (MSI), can occur in several human
78 cancers, but is more frequently observed in colorectal, endometrial and gastric tumors (1, 2).
79 Until recently, MMR status testing was performed in the context of newly diagnosed
80 colorectal cancers and as a first screening tool in cancers suspected to be related to Lynch
81 syndrome, an inherited cancer predisposition condition associated with MMR deficiency and
82 MSI cancer formation (3-5). Following the approval of pembrolizumab (anti-programmed cell
83 death-1) in 2017 for the treatment of unresectable or metastatic MSI solid tumors, MSI testing
84 became critical for all advanced cancers regardless of their tissue of origin (6-9).
85 Routine clinical testing relies on immunohistochemistry of MMR machinery components
86 (mutL homolog 1 [MLH1], mutS homolog 2 [MSH2], mutS homolog 6 [MSH6], and PMS1
87 homolog 2 [PMS2]) and PCR amplification of reference microsatellite markers, followed by
88 capillary electrophoresis (4). The presence of alleles in the tumor that are not found in
89 matched normal tissue are indicative of MSI. The most widely used commercial kit, referred
90 to as the “pentaplex assay”, interrogates 5 microsatellite markers (BAT-25, BAT-26, NR-21,
91 NR-24, and MONO-27), comprising stretches of 21 to 27 poly-A repeats. Tumors with
92 instability in two or more markers are classified as MSI, whereas those with one or no
93 detectable alterations are classified as microsatellite stable (MSS). This panel has good
94 clinical sensitivity for MSI status characterization in Lynch-spectrum tumors (10, 11).
95 However, its relevance for MSI status characterization in other tumor types is largely
96 unknown. Recently, algorithms that can detect MSI using next-generation sequencing (NGS)
97 data were developed (1, 2, 11-13). Such approaches showed that MSI is much more prevalent
98 than previously thought. For example, using exome sequencing data to investigate more than

99 200,000 microsatellites, Hause et al. identified MSI in 14 different cancer types, including
100 those with low MSI incidence (*1*). Moreover, these studies have also identified new highly
101 informative MSI markers, opening avenues for the development of panels more relevant for
102 cancer types not classically associated with MSI.

103 The current trend towards systematic detection of MSI in metastatic cancer patients has also
104 stimulated the development of non-invasive diagnostic methods capable of detecting MSI in
105 circulating tumor DNA (ctDNA). Such strategies require methodologies with high sensitivity,
106 capable of detecting abnormal MSI alleles highly diluted in fragmented DNA from normal
107 cells. Here, we describe for the first time a quantitative droplet-digital PCR (ddPCR) approach
108 for highly sensitive detection of MSI (<0.1% mutant allelic frequency or MAF). The method
109 is compatible with both tissue and body fluid samples and provides a cost-effective, simple
110 and fast diagnostic tool for the high-throughput screening of patients and the monitoring of
111 responses to therapy.

112 **Materials and methods**113 *Cell lines and clinical samples*

114 Human cancer cell lines HCT-116, HCT-15 and LoVo were used as MSI positive controls.

115 SW480, SW1116, PSN1, and buffy coat from healthy donors were used as MSS controls.

116 Genomic and cell-free DNA (cfDNA) were extracted using the QIAamp DNA mini and

117 Circulating Nucleic Acid Kits, respectively. Archived clinical samples were retrieved from

118 Institut Curie Pharmacogenomics. A waiver of informed consent was obtained given the

119 retrospective nature of the study. Plasma samples from healthy donors were obtained from

120 *Etablissement Français du Sang*, under French and European ethical practices.

121

122 *ddPCR conditions and data analysis*

123 Primers and probes are described in online Supplemental Table 1. The *KRAS* proto-oncogene

124 (*KRAS*) drop-off assay is described elsewhere (14). The *KRAS*^{Q61L} assay was ordered from

125 BioRad. ddPCR reactions were performed using the Bio-Rad QX100, with 900 nM of each

126 primer, 250 nM of each probe, up to 5000 genome equivalents of DNA, and under the

127 following conditions : 95°C for 10 min followed by 40 cycles of 94°C for 30 s, 61°C for 3

128 min (BAT-26) or 59°C for 3 min (defensin beta 105A/B [*DEFB105A/B*]) or 55°C for 3 min

129 (activin A receptor type 2A [*ACVR2A*]) or 60°C for 1 min (*B-RAF* proto-oncogene

130 [*BRAF*^{V600E}] and phosphatidylinositol-4,5-bisphosphate 3-kinase catalytic subunit alpha

131 [*PIK3CA*^{H1047R}]) or 63°C for 1 min (*KRAS*^{G12/13}) or 55°C for 1 min (*KRAS*^{Q61L}); final hold at

132 98°C for 10 min. Cluster thresholding and quantification were performed with QuantaSoft

133 v1.7.4. For the drop-off assays, droplets were manually assigned as wild type (WT) or mutant

134 based on their fluorescence amplitude: WT=VIC⁺/FAM⁺; MSI mutant=VIC⁺/FAM^{-low} and

135 mutant *KRAS*=VIC^{-low}/FAM⁺. Samples were run in one or multiple replicates depending on

136 sample availability, cfDNA concentration and ctDNA fraction. Samples were considered to be

137 positive if at least one replicate presented ≥ 2 positive MSI droplets and if the mean MAF was
138 higher than the defined limit of detection (LOD) of each assay.

139

140 *Limit of blank (LOB) and LOD*

141 The false-positive rate of each assay was estimated using ≥ 53 replicates of WT DNA. The
142 LOB was defined as the upper 95% confidence limit of the mean false-positive
143 measurements. The analytical sensitivity was estimated using serial dilutions of HCT-116 in
144 WT DNA, with MAFs ranging from 10% to 0.01%. The number of replicates per dilution
145 point ranged from 3 to 8. LOD was estimated as the lowest mutant concentration that could be
146 reliably distinguished from the LOB (14, 15).

147

148 *Statistical analysis*

149 The discriminatory power of each marker was investigated using receiver operating
150 characteristic analyses. Areas under the curve were: 0.95 (95% confidence interval, 0.9-0.99)
151 for BAT-26 and 0.99 (0.99-1) for ACVR2A and DEFB105A/B. Optimized cut-offs were
152 calculated to minimize classification errors. Analytical sensitivity and specificity for the
153 chosen cut-offs were: 99% [confidence interval, 88%-100%] and 95% [96%-99%] for BAT-
154 26, 99% [96%-100%] and 100% for ACVR2A, and 99% [96%-100%] and 96% [91%-100%]
155 for DEFB105A/B, respectively. Global error rates were 3.2% for BAT-26, 0.8% for ACVR2A
156 and 2.4% for DEFB105A/B.

157

158 **Results**

159 *Proof of principle*

160 We recently described drop-off ddPCR strategies for the accurate detection and quantification
161 of all nucleotide variations present in a given region, for example in *KRAS* exon 2 and *EGFR*
162 exon 19 hotspots (14). The drop-off ddPCR method relies on the design of two hydrolysis

163 probes within the same PCR fragment. The reference probe (REF) is complementary to a non-
164 variable region, and the target probe (DROP-OFF) is complementary to the WT sequence of
165 the hotspot region where mutations are frequently observed. The presence of variants in the
166 hotspot region results in a mismatch with the DROP-OFF probe and the absence of hydrolysis
167 during amplification. Therefore, in a drop-off ddPCR assay three clusters of droplets can be
168 observed: droplets with no template (REF/DROP-OFF⁻), droplets containing WT alleles
169 (REF⁺/DROP-OFF⁺) and droplets containing mutant alleles (REF⁺/DROP-OFF^{-/low}).

170 We predicted that such drop-off ddPCR strategy could be instrumental to detect the
171 microsatellite length variations that characterize MSI tumors. To determine the feasibility of
172 this approach, we first developed an assay targeting the BAT-26 reference microsatellite, one
173 of the five markers of the pentaplex assay (10, 16). The BAT-26 assay included a VIC-labeled
174 REF probe and a FAM-labeled drop-off probe (MSI probe), which covered the entire A27
175 homopolymer plus 4 and 2 bases upstream and downstream of the repeat, respectively (Figure
176 1A). After adjustments of the annealing temperature and extension time, we reached a clear
177 separation between WT and MSI droplet clouds (Figure 1). The assay could specifically
178 detect MSI in DNA from the MSI colorectal cancer (CRC) cell lines HCT-116 and HCT-15,
179 which carry shortened BAT-26 alleles (Figure 1B and online Supplemental Figure 1A).

180 Although the separation of the WT and MSI-positive clouds was clear in both cell lines, it was
181 less pronounced for HCT-15 (3 nucleotide [nt] deletion) than for HCT-116 (12 nt deletion),
182 suggesting a low level of non-specific binding of the MSI probe to BAT-26 alleles containing
183 short deletions (Figure 1B). It is noteworthy that no instability was observed in DNA from
184 MSS cell lines, such as the CRC cell lines SW480 and SW1116 or the pancreatic cancer cell
185 line PSN1.

186 To demonstrate the flexibility of the MSI-ddPCR approach, we next developed assays
187 targeting the two most discriminatory microsatellite markers associated with MSI-H cancers

188 identified by Hause *et al.* (1). The two loci comprised the A8 and A9 repeats located within
189 the *ACVR2A* gene and *DEFB105 A* and *B* paralogous genes, respectively. These shorter
190 markers usually show deletions of only 1 or 2 nt and are difficult to interrogate with the PCR-
191 capillary electrophoresis approach. Similar to what was observed for BAT-26, the *ACVR2A*
192 and *DEFB105A/B* assays specifically detected MSI in HCT-116 and HCT-15, while no
193 instability was observed in MSS cell lines (Figure 1B and online Supplemental Figure 1).
194 Moreover, both assays detected MSI in the LoVo CRC cell line, which carries a homozygous
195 deletion encompassing the BAT-26 marker (online Supplemental Figure 1B and C). The
196 *DEFB105A/B* assay discriminates MSI alleles with different deletion sizes, as observed for
197 HCT-116 and LoVo, which harbor MSI alleles shortened by 1 nt and 2 nt (online
198 Supplemental Figure 1C). For *ACVR2A*, MSI alleles shortened by a single nt were observed in
199 the three cell lines (Supplemental Figure 1C). Remarkably, the three assays accurately
200 quantified MSI in 1/2 and 1/10 dilutions of HCT-116, HCT-15 and LoVo DNA in WT DNA
201 (online Supplemental Figure 1D). Indeed, MAFs quantified by MSI-ddPCR assays correlated
202 with $r \geq 0.99$ ($p < 0.001$) with the ones reported by a commercial ddPCR assay that targets
203 *KRAS*^{G13D}, a heterozygous mutation shared by the three cell lines. Taken together, these
204 results demonstrate the feasibility of developing ddPCR assays targeting long and short
205 repetitive regions of the genome and its applicability to MSI status determination and accurate
206 quantification.

207

208 *Analytical sensitivity for MSI detection and quantification accuracy*

209 We subsequently used serial dilutions ranging from 10% to 0.01% of HCT-116 DNA in WT
210 DNA and pure WT DNA to estimate the analytical sensitivity of each MSI-ddPCR assay. The
211 LOB was estimated at 0.01% for the three assays (online Supplemental Figure 2A, online
212 Supplemental Table 2). The LOD was found to be 0.04% for BAT-26 and 0.08% for both

213 *ACVR2A* and *DEFB105A/B* markers (online Supplemental Figure 2B-D). For the three assays,
214 the Pearson's correlations were $r=0.99$ $p<0.0001$ between the expected and observed MAFs,
215 suggesting the accurate quantification of MSI alleles at a wide range of allelic frequencies.
216 This *in vitro* performance of the MSI ddPCR assays prompted us to assess their efficiency in
217 clinical samples.

218

219 *Comparison MSI-ddPCR versus pentaplex-PCR*

220 *BAT-26*, *ACVR2A* and *DEFB105A/B* markers are recurrently unstable among MSI CRC
221 samples (1, 11, 16). To test the clinical sensitivity of this 3-marker panel for detection of MSI
222 in this cancer type, we blindly tested a series of 126 formalin-fixed paraffin-embedded
223 (FFPE) samples previously classified as MSI (n=70) or MSS (n=56) using the pentaplex test
224 and immunohistochemistry (IHC) for the 4 major MMR machinery components (online
225 Supplemental Table 2, FFPE-1 to 126). As expected, MSI MAFs estimated by MSI-ddPCR
226 assays showed a bimodal distribution, concordant with the MSI status reported for these
227 samples (Figure 2A and online Supplemental Tables 3 and 4, FFPE-1 to 126). Median MAFs
228 obtained for MSI and MSS samples were 41% (interquartile range, 30%-54%) and 0% (0%-
229 0%) for *BAT-26*; 36% (23%-48%) and 0.08% (0%-0.2%) for *ACVR2A*; and 21% (17%-29%)
230 and 0.13% (0%-0.4%) for *DEFB105A/B*, respectively. Conversely, MAFs estimated by
231 ddPCR assays targeting known *BRAF* (n=34), *KRAS* (n=23) or *PIK3CA* (n=1) tumor
232 mutations displayed a unimodal distribution among MSI and MSS samples, with median
233 values of 22% (16%-29%). Using receiver operating characteristic analyses, we next
234 determined optimized MAF cut-offs of $\geq 6\%$ for *BAT-26* and $\geq 1.2\%$ for both *ACVR2A* and
235 *DEFB105A/B* to classify these markers as unstable. Considering a sample as MSI when at
236 least 2 markers were reported as unstable, the 3-marker MSI-ddPCR test achieved 100%
237 clinical sensitivity and 100% clinical specificity in comparison with the pentaplex

238 classification (online Supplemental Table 3). This criterion was used in order to avoid
239 misclassification of MSS samples as MSI due to germline polymorphisms, as observed for
240 BAT-26 in samples FFPE-55, 65 and 91 (online Supplemental Table 3). Finally, we tested an
241 additional sample (FFPE-127) corresponding to a metastatic tumor highly infiltrated by
242 lymphocytes (cellularity < 10%). This sample was classified as dMMR by IHC (loss of
243 expression of MSH2 and MSH6), but as MSS by pentaplex PCR. MSI-ddPCR results
244 supported the MSI phenotype with MAFs close to the defined thresholds (BAT-26, *ACVR2A*
245 and *DEFB105A/B* markers at 2.9%, 2.5% and 0.8% MAF, respectively; online Supplemental
246 Tables 3 and 4), which could be explained by the higher analytical sensitivity of this
247 approach.

248 Based on these results, we concluded that the 3-marker MSI-ddPCR performed as well as the
249 pentaplex-PCR for MSI status characterization in CRC, with the additional advantage of
250 allowing MSI testing in tumor samples highly contaminated with WT DNA.

251 We next evaluated the assay ability to detect MSI in other tumor types. We screened a
252 collection of 59 previously characterized FFPE samples (25 MSI and 34 MSS), including
253 endometrial (20 MSI and 28 MSS), ovarian carcinomas (1 MSI and 3 MSS), sebaceoma (1
254 MSI), cholangiocarcinoma (1 MSI), gastric carcinoma (1 MSI), small bowel adenocarcinoma
255 (1 MSI), pancreatic ductal adenocarcinomas (2 MSS) and appendix carcinoma (1 MSS)
256 (Figure 2B and online Supplemental Tables 3 and 4, FFPE-128 to 186). Using the criteria
257 described above, we found concordant results between the pentaplex-PCR and the 3-marker
258 MSI-ddPCR. 92% of the samples defined as MSI by the pentaplex test were classified as MSI
259 by MSI-ddPCR (23/25), whereas all the MSS samples were correctly classified as MSS. We
260 further evaluated 8 additional samples (endometrial carcinoma, n=4; ovarian carcinoma, n=1;
261 chordoma, n=1; glioma, n=1; glioblastoma, n=1) that were classified as dMMR by IHC but
262 MSS by pentaplex PCR. As expected, BAT-26 was reported stable by MSI-ddPCR in these 8

263 samples. However, MSI was detected at *ACVR2A* and *DEFB105A/B* markers in 4 and 5
264 samples, respectively (online Supplemental Tables 3 and 4). Taken together, these results
265 supported the development of assays targeting additional markers identified by cancer exome
266 sequencing data to improve the clinical sensitivity of MSI testing for different cancer types.

267

268 *Quantification of tumor content by MSI-ddPCR*

269 One of the advantages of ddPCR over the standard pentaplex-PCR is its quantitative
270 capability. Using the data obtained for the 40 MSI CRC samples mutated for *BRAF* (n=31),
271 *KRAS* (n=8) or *PIK3CA* (n=1) oncogenes (Figure 2A; online Supplemental Tables 3 and 4),
272 we evaluated the correlation between MAFs estimated by MSI-ddPCR assays and the ones
273 reported by ddPCR assays targeting these mutations. Pearson's correlations of $r=0.78$ and
274 $r=0.7$, respectively; $p<0.0001$ (Figure 2C) were observed for the BAT-26 and *ACVR2A*
275 markers, which accurately estimated the tumor fraction. No correlation was found for
276 *DEFB105A/B* across the different samples (Pearson's $r=0.25$ $p=0.12$; Figure 2C), which may
277 be explained by frequent variations in the number of copies of the *DEFB105* genes among
278 individuals (2 to 12 per haploid genome) (17), or by clonal heterogeneity of *DEFB105*
279 instability. Taken together, these results supported the utility of the MSI-ddPCR assays for
280 accurate quantification of tumor fractions in patient samples.

281

282 *MSI status characterization and tumor fraction in blood samples by MSI-ddPCR*

283 MSI-ddPCR is a highly clinically sensitive and quantitative assay. We thus hypothesized that
284 it would be relevant as a liquid biopsy tool to simultaneously detect MSI and quantify ctDNA.
285 We therefore characterized 30 archival blood samples (plasma or serum) collected at baseline
286 and/or during treatment from 14 patients with locally advanced or metastatic CRC or
287 endometrial tumors, defined as MSI by the pentaplex assay. The three ddPCR assays detected

288 MSI in blood samples from all the patients tested (online Supplemental Figure 3, online
289 Supplemental Tables 5 and 6). Moreover, for patients with *BRAF* or *PIK3CA* mutated tumors
290 (P1, P2, P4, P5, and P8), ctDNA fractions quantified by the MSI-ddPCR assays were
291 validated by ddPCRs specifically targeting these mutations (*BRAF*^{V600E} and *PIK3CA*^{H1047R},
292 Pearson's $r=0.99$ $p<0.0001$, Figure 3B, online Supplemental Tables 5 and 6). These results
293 supported the reliability of the MSI-ddPCR assays for accurate ctDNA quantification. Indeed,
294 for patients with sequential samples collected at baseline and at different time points during
295 treatment, ctDNA kinetics estimated by MSI-ddPCR assays mirrored the tumor response to
296 therapy (Figure 3A). Of note, patients P1, P4, P5, P6, and P7 were treated with
297 pembrolizumab. Strikingly, patients P1, P4, and P7 responded to pembrolizumab and showed
298 undetectable or dramatically decreased ctDNA concentrations (>90% MAF decrease) over the
299 first weeks of treatment. On the other hand, patients P5 and P6 did not respond to therapy and
300 showed increased or stable ctDNA concentrations. Similarly, decreased ctDNA
301 concentrations for the patient P9 followed well the patient's partial response to chemo-
302 radiotherapy (Figure 3A). Finally, when the MSI-ddPCR assays were applied to 38 serum and
303 4 plasma samples collected from 28 patients with advanced MSS tumors, none of the samples
304 were positive for MSI, even though 74% (29/39) of the samples from patients with *KRAS*
305 (n=21) or *BRAF* (n=5) mutated tumors were positive for ctDNA (*KRAS* or *BRAF* median
306 MAF 4.2%, min=0.2%, max=71.4%). Similarly, plasma samples collected from healthy
307 donors (n=48) were all negative for MSI, yielding a clinical specificity of 100% (online
308 Supplemental Tables 5 and 6). Based on these data, we concluded that the MSI-ddPCR assays
309 were both highly clinically sensitive and specific, as well as suitable for the quantitative
310 detection of ctDNA in longitudinal studies.

311 **Discussion**

312 Here we present a new ddPCR test for fast, clinically sensitive and cost-effective detection of
313 MSI. Most importantly, the high analytical and clinical sensitivity reached by this method
314 allows for its use as a liquid biopsy tool to simultaneously detect MSI and quantify ctDNA.
315 The method is also well suited to screen FFPE tumors and does not require matched normal
316 samples for reliable MSI identification. As a proof-of-concept, we set up ddPCR assays
317 targeting the microsatellites located inside *MSH2* (BAT-26), *ACVR2A* and *DEFB105A/B*
318 genes. While BAT-26 is one of the five NCI reference markers widely used in clinical
319 practice, *ACVR2A* and *DEFB105A/B* are novel discriminatory markers identified as frequently
320 unstable among MSI cancers (1, 2). As expected based on the frequent instability of these
321 markers in CRC (1, 11, 16), the MSI-ddPCR test showed 100% concordance with the
322 reference pentaplex assay for MSI status characterization in this cancer type. The concordance
323 decreased to 90% for endometrial cancers, with both panels failing to classify all dMMR
324 samples as MSI (20/24 correctly classified as MSI by pentaplex and 21/24 by MSI-ddPCR).
325 Indeed, pan-cancer identification of MSI remains challenging when using reduced panels of
326 markers. This limitation is currently being addressed by more comprehensive NGS-based
327 approaches (1, 2, 11-13). A recent study reported the use of a 98-kb pan-cancer panel, which
328 included microsatellites, to detect MSI in blood (18). With a panel of 99 microsatellite
329 sequences, Willis *et al.* described MSI detection across 16 cancer types (19). However, NGS
330 assays are costly and time-consuming when compared to targeted approaches such as MSI-
331 ddPCR. Moreover, MSI-ddPCR achieved 100% clinical sensitivity in blood samples
332 compared to 87% (19) and 78% (18) for the above studies. MSI-ddPCR is therefore more
333 suitable for routine clinical practice screening and monitoring of response to treatment.
334 Systematic investigation of MSI in cancer exomes has uncovered shared and cancer-type
335 specific patterns of instability and therefore is setting the ground for future development of

336 more sensitive panels of markers (1, 2, 11-13). In this context, MSI-ddPCR stands as a
337 promising approach for the next generation of panel-based MSI tests. Indeed, the method
338 provides robust direct measurements of MSI for both long non-coding markers (such as BAT-
339 26), as well as for coding microsatellites (such as ACVR2A), which usually show indels of
340 only a single nucleotide. Therefore, MSI-ddPCR should be easily adapted to different panels
341 of markers, depending on the clinical need, and could help to improve MSI testing in
342 extracolonic tumors for which the reference pentaplex panel has more limited clinical
343 sensitivity. Moreover, high order multiplexing of ddPCR assays should become feasible with
344 the release of multicolor digital PCR platforms.

345 The analytical sensitivity of MSI-ddPCR is at least 2 orders of magnitude higher than the
346 detection threshold of the reference pentaplex method ($\geq 10\%$ MAF) (20, 21), opening up the
347 possibility of non-invasive MSI detection in ctDNA. CtDNA has demonstrated its clinical
348 value as a liquid biopsy tool (22, 23), and has been approved in metastatic non-small cell lung
349 cancer as a non-invasive surrogate to tumor biopsies for the detection of activating *EGFR*
350 mutations (24). In face of the unprecedented approval of anti-checkpoint inhibitors for the
351 treatment of metastatic solid tumors regardless of tumor site, a similar situation could be
352 envisaged for MSI (6-9). Recently, an alternative strategy was proposed for highly sensitive
353 MSI detection (21). The method uses targeted nuclease digestion to enrich for altered
354 microsatellite sequences prior to PCR amplification. This procedure reduces confounding
355 stutter bands generated by amplification of unaltered microsatellites, therefore increasing the
356 resolution of fragment analysis. However, pre-analytic enrichment renders this approach non-
357 quantitative. MSI-ddPCR in contrast provides absolute quantification of MSI alleles and
358 therefore is also suitable for other clinical applications of ctDNA, including patient follow-up
359 (25). We anticipate that MSI-ddPCR will prove its usefulness for the monitoring of immune

360 checkpoint inhibitor efficacy. Early detection of non-responders should improve patient
361 management and significantly reduce costs for the healthcare system.

362 In summary, MSI-ddPCR allows robust, non-invasive detection of MSI with high clinical
363 sensitivity. The method is straightforward and has the potential to be routinely applied
364 clinically in laboratories equipped with a digital PCR platform. MSI-ddPCR is compatible
365 with high throughput screening of patients, including those with cancers with low MSI
366 prevalence, promising increased access to personalized treatments.

367

368 **Acknowledgements:** We thank Aurore Rampanou, Caroline Hego, Chloe Derouet, Pascal
369 Portois and Frederique Maraone for invaluable technical support. We thank Charles Decraene
370 and Olivier Lantz for discussions and Christopher R Muller for critical reading of the
371 manuscript. We also thank the group of Valérie Taly for providing us with MSI cell lines
372 (LoVo, HCT-15).

373 **Author contributions:** ABS, FCB, CP and MHS designed the study. ABS and AK performed
374 experiments. ABS, FCB, CP and MHS analyzed data. MLT performed the statistical analysis.
375 ABS, FCB, SM, GB, LC, BB and JYP contributed with identification of clinical samples.
376 ABS wrote the manuscript with support of FCB, CP and MHS.

377 **Disclosure/Conflict of interest:** ABS, FCB, AK, CP and MHS are inventors on a patent
378 application submitted by the Institut Curie (PCT/ EP 2018/068760). The other authors declare
379 no competing financial interests. This work was supported by SiRIC1 Curie (grant INCa-
380 DGOS-Inserm_4654), SiRIC2 Curie (grant INCa-DGOS-Inserm_12554), and the Innovative
381 Medicines Initiative Joint Undertaking under grant agreement no. 115749 (project Cancer-
382 ID).

383

384 **References**

- 385 1. Hause RJ, Pritchard CC, Shendure J, Salipante SJ. Classification and characterization of
386 microsatellite instability across 18 cancer types. *Nat Med* 2016;22:1342-50.
- 387 2. Cortes-Ciriano I, Lee S, Park WY, Kim TM, Park PJ. A molecular portrait of microsatellite
388 instability across multiple cancers. *Nat Commun* 2017;8:15180.
- 389 3. Umar A, Risinger JI, Hawk ET, Barrett JC. Testing guidelines for hereditary non-polyposis
390 colorectal cancer. *Nat Rev Cancer* 2004;4:153-8.
- 391 4. Buza N, Ziai J, Hui P. Mismatch repair deficiency testing in clinical practice. *Expert Rev*
392 *Mol Diagn* 2016;16:591-604.
- 393 5. Latham A, Srinivasan P, Kemel Y, Shia J, Bandlamudi C, Mandelker D, et al.
394 Microsatellite instability is associated with the presence of lynch syndrome pan-
395 cancer. *J Clin Oncol* 2019;37:286-95.
- 396 6. Le DT, Durham JN, Smith KN, Wang H, Bartlett BR, Aulakh LK, et al. Mismatch repair
397 deficiency predicts response of solid tumors to pd-1 blockade. *Science* 2017;357:409-
398 13.
- 399 7. Overman MJ, McDermott R, Leach JL, Lonardi S, Lenz HJ, Morse MA, et al. Nivolumab
400 in patients with metastatic DNA mismatch repair-deficient or microsatellite instability-
401 high colorectal cancer (checkmate 142): An open-label, multicentre, phase 2 study.
402 *Lancet Oncol* 2017;18:1182-91.
- 403 8. Overman MJ, Lonardi S, Wong KYM, Lenz HJ, Gelsomino F, Aglietta M, et al. Durable
404 clinical benefit with nivolumab plus ipilimumab in DNA mismatch repair-
405 deficient/microsatellite instability-high metastatic colorectal cancer. *J Clin Oncol*
406 2018;36:773-9.

- 407 9. Kim ST, Cristescu R, Bass AJ, Kim KM, Odegaard JI, Kim K, et al. Comprehensive
408 molecular characterization of clinical responses to pd-1 inhibition in metastatic gastric
409 cancer. *Nat Med* 2018;24:1449-58.
- 410 10. Bacher JW, Flanagan LA, Smalley RL, Nassif NA, Burgart LJ, Halberg RB, et al.
411 Development of a fluorescent multiplex assay for detection of msi-high tumors. *Dis*
412 *Markers* 2004;20:237-50.
- 413 11. Maruvka YE, Mouw KW, Karlic R, Parasuraman P, Kamburov A, Polak P, et al. Analysis
414 of somatic microsatellite indels identifies driver events in human tumors. *Nat*
415 *Biotechnol* 2017;35:951-9.
- 416 12. Bonneville R, Krook MA, Kautto EA, Miya J, Wing MR, Chen HZ, et al. Landscape of
417 microsatellite instability across 39 cancer types. *JCO Precis Oncol* 2017;2017.
- 418 13. Middha S, Zhang L, Nafa K, Jayakumaran G, Wong D, Kim HR, et al. Reliable pan-
419 cancer microsatellite instability assessment by using targeted next-generation
420 sequencing data. *JCO Precis Oncol* 2017;2017.
- 421 14. Decraene C, Silveira AB, Bidard FC, Vallee A, Michel M, Melaabi S, et al. Multiple
422 hotspot mutations scanning by single droplet digital pcr. *Clin Chem* 2018;64:317-28.
- 423 15. Bidshahri R, Attali D, Fakhfakh K, McNeil K, Karsan A, Won JR, et al. Quantitative
424 detection and resolution of braf v600 status in colorectal cancer using droplet digital
425 pcr and a novel wild-type negative assay. *J Mol Diagn* 2016;18:190-204.
- 426 16. Suraweera N, Duval A, Reperant M, Vaury C, Furlan D, Leroy K, et al. Evaluation of
427 tumor microsatellite instability using five quasimonomorphic mononucleotide repeats
428 and pentaplex pcr. *Gastroenterology* 2002;123:1804-11.
- 429 17. Hollox EJ, Armour JA, Barber JC. Extensive normal copy number variation of a beta-
430 defensin antimicrobial-gene cluster. *Am J Hum Genet* 2003;73:591-600.

- 431 18. Georgiadis A, Durham JN, Keefer LA, Bartlett BR, Zielonka M, Murphy D, et al.
432 Noninvasive detection of microsatellite instability and high tumor mutation burden in
433 cancer patients treated with pd-1 blockade. *Clin Cancer Res* 2019;25:7024-34.
- 434 19. Willis J, Lefterova MI, Artyomenko A, Kasi PM, Nakamura Y, Mody K, et al. Validation
435 of microsatellite instability detection using a comprehensive plasma-based genotyping
436 panel. *Clin Cancer Res* 2019;25:7035-45.
- 437 20. Lee HS, Kim WH, Kwak Y, Koh J, Bae JM, Kim KM, et al. Molecular testing for
438 gastrointestinal cancer. *J Pathol Transl Med* 2017;51:103-21.
- 439 21. Ladas I, Yu F, Leong KW, Fitarelli-Kiehl M, Song C, Ashtaputre R, et al. Enhanced
440 detection of microsatellite instability using pre-pcr elimination of wild-type DNA
441 homo-polymers in tissue and liquid biopsies. *Nucleic Acids Res* 2018;46:e74.
- 442 22. Alix-Panabieres C, Pantel K. Clinical applications of circulating tumor cells and
443 circulating tumor DNA as liquid biopsy. *Cancer Discov* 2016;6:479-91.
- 444 23. Siravegna G, Marsoni S, Siena S, Bardelli A. Integrating liquid biopsies into the
445 management of cancer. *Nat Rev Clin Oncol* 2017;14:531-48.
- 446 24. Douillard JY, Ostoros G, Cobo M, Ciuleanu T, Cole R, McWalter G, et al. Gefitinib
447 treatment in egfr mutated caucasian nscl: Circulating-free tumor DNA as a surrogate
448 for determination of egfr status. *J Thorac Oncol* 2014;9:1345-53.
- 449 25. Cabel L, Proudhon C, Romano E, Girard N, Lantz O, Stern MH, et al. Clinical potential of
450 circulating tumour DNA in patients receiving anticancer immunotherapy. *Nat Rev*
451 *Clin Oncol* 2018;15:639-50.
- 452
- 453

454 **Figure Captions**

455

456 **Figure 1. Microsatellite instability (MSI)-ddPCR drop-off assays.** A. Schematic
457 representation of the principle of the method. B. 2-D scatter plots of BAT-26, *ACVR2A* and
458 *DEFB105A/B* assays using 10% dilutions of HCT-116 or HCT-15 MSI CRC cell lines in WT
459 DNA. Droplets containing wild type (WT), MSI alleles and no DNA template are indicated as
460 blue, green and gray clusters, respectively.

461

462 **Figure 2. Microsatellite instability (MSI) status characterization in tumor specimens by**
463 **MSI-ddPCR.** Distribution of MSI allelic frequencies measured by BAT-26, *ACVR2A* and
464 *DEFB105A/B* assays in colorectal carcinoma (CRC) (A) or non-CRC tumors (B). Black and
465 red dots represent samples classified as MSI or microsatellite stable (MSS) by the pentaplex
466 test, respectively. Optimized thresholds were calculated using receiver operating
467 characteristics analysis. (C) Correlation between mutant allele frequencies (MAFs) measured
468 by MSI-ddPCR and *BRAF*^{V600E}, *KRAS*^{G12/13} or *PIK3CA*^{H1047R} dPCR assays.

469

470 **Figure 3. Microsatellite instability (MSI) detection in blood samples of advanced cancer**
471 **patients by MSI-ddPCR.** A. ctDNA dynamics in blood samples at baseline (B) and during
472 treatment (M: month, W: week). Arrows indicate associated responses based on CT scans
473 (PR: partial response, SD: stable disease, PD: progressive disease). B. Correlation between
474 ctDNA fractions estimated by MSI-ddPCR assays and ddPCR assays specifically targeting
475 *BRAF*^{V600E} or *PIK3CA*^{H1047R} mutations for patients (P) 1, 2, 4, 5, and 8.

476

Fig. 1

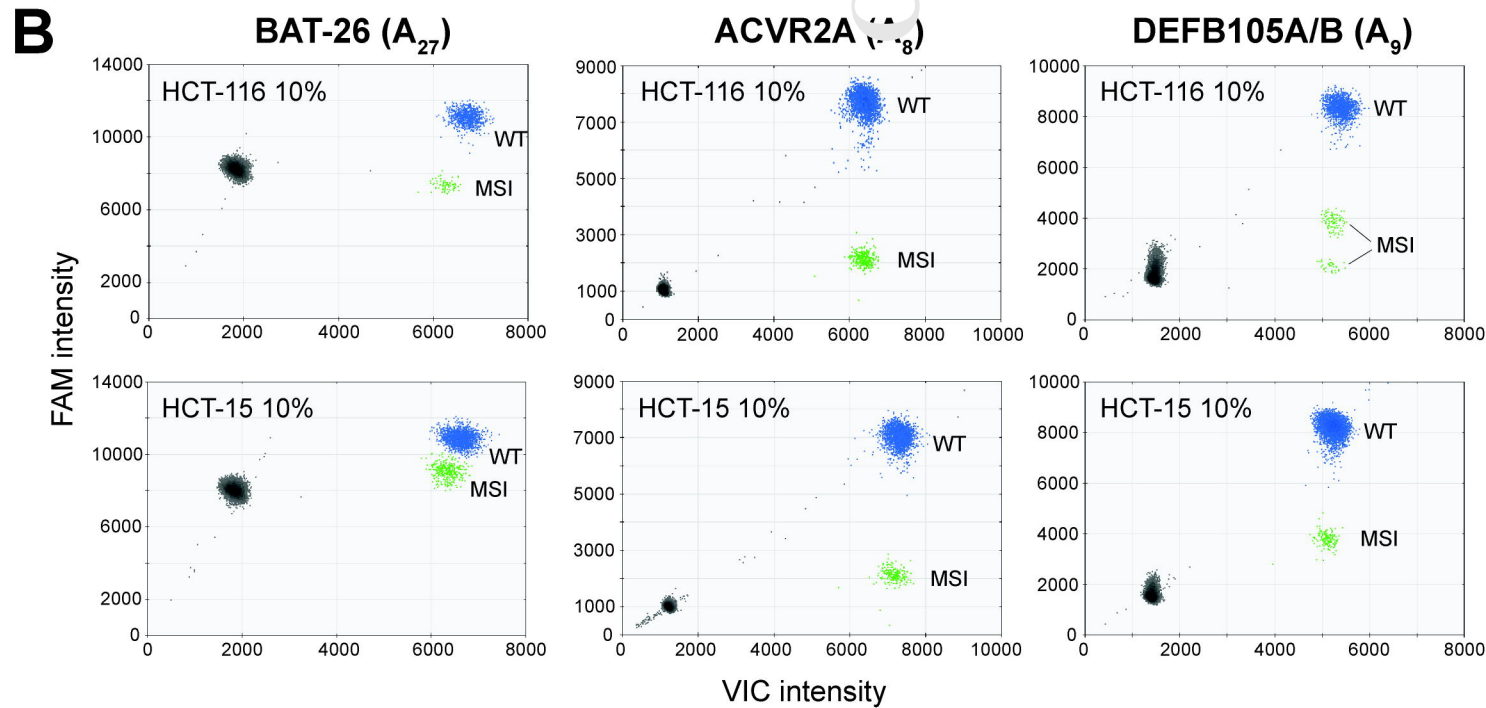
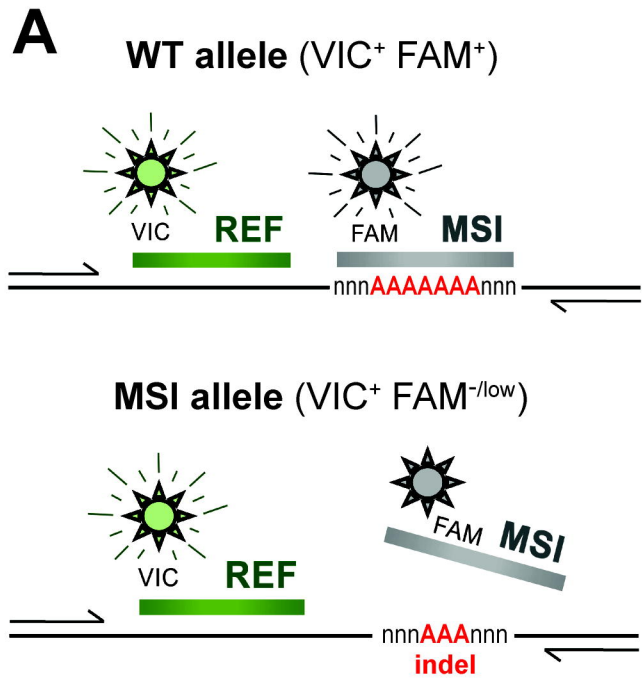


Fig. 2

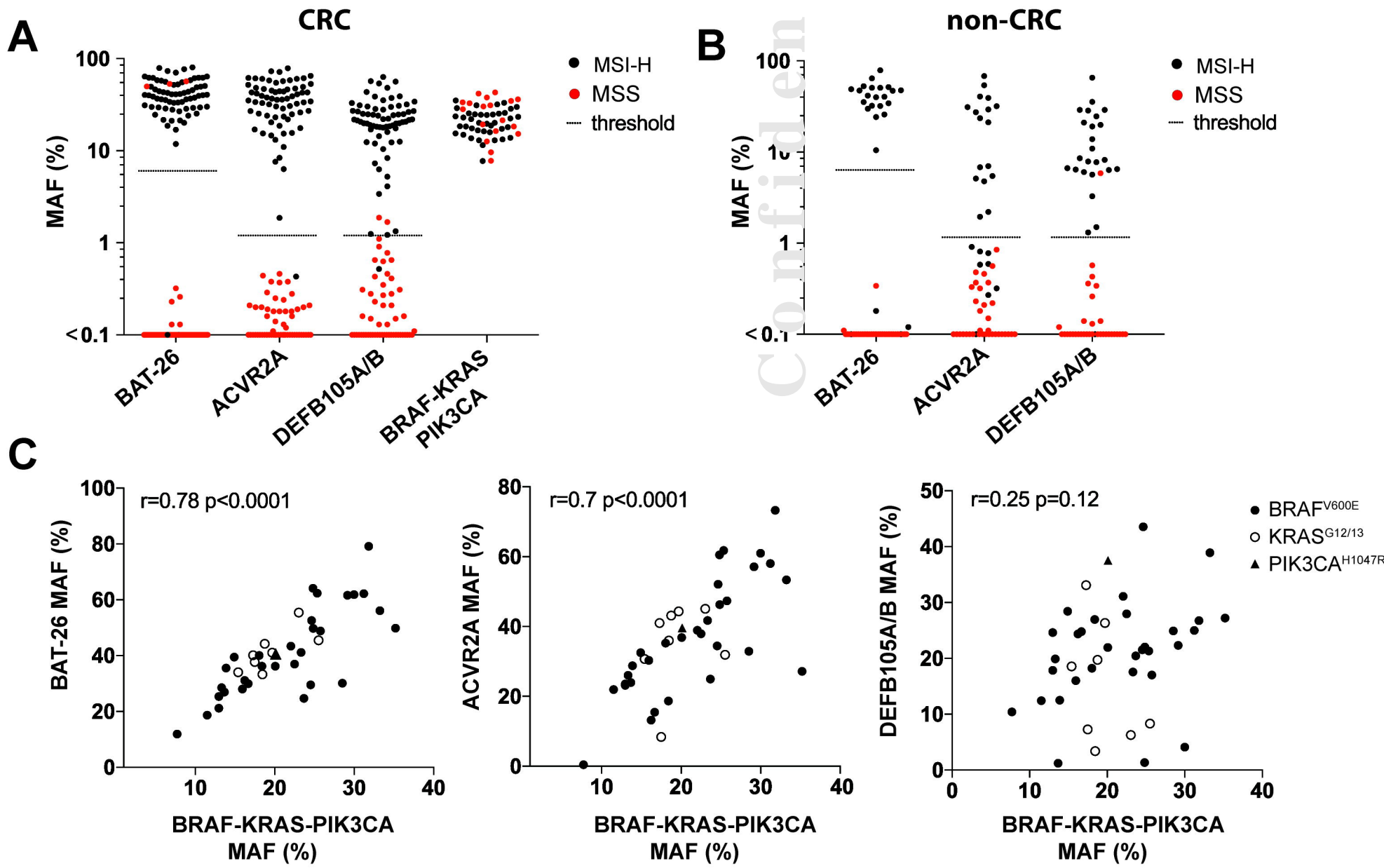
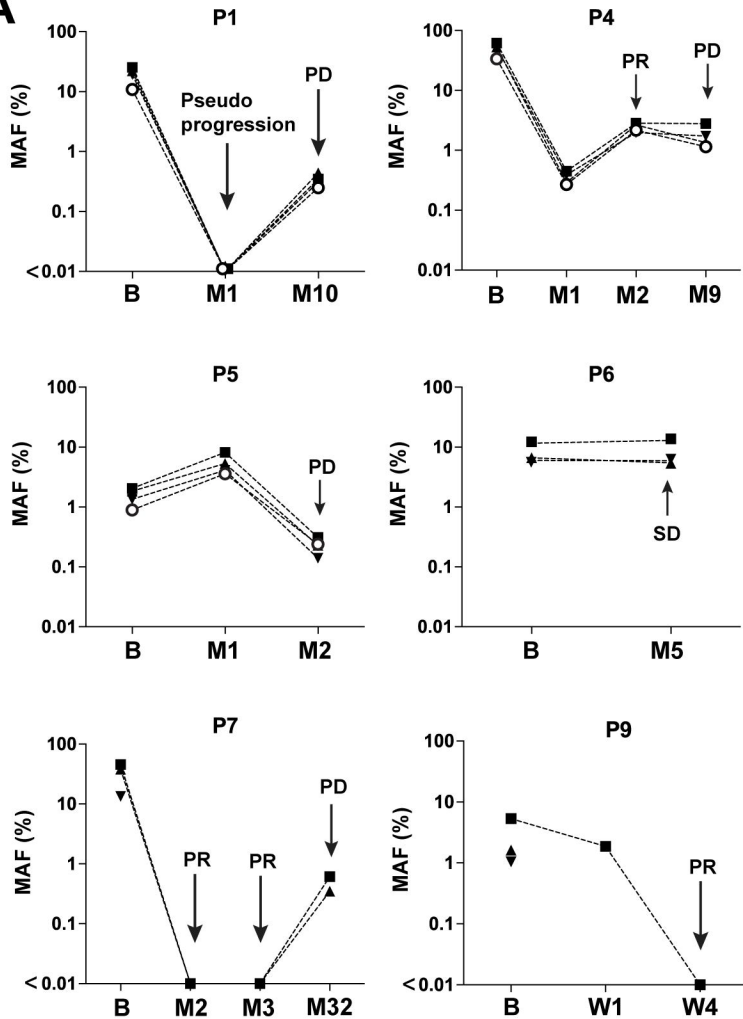
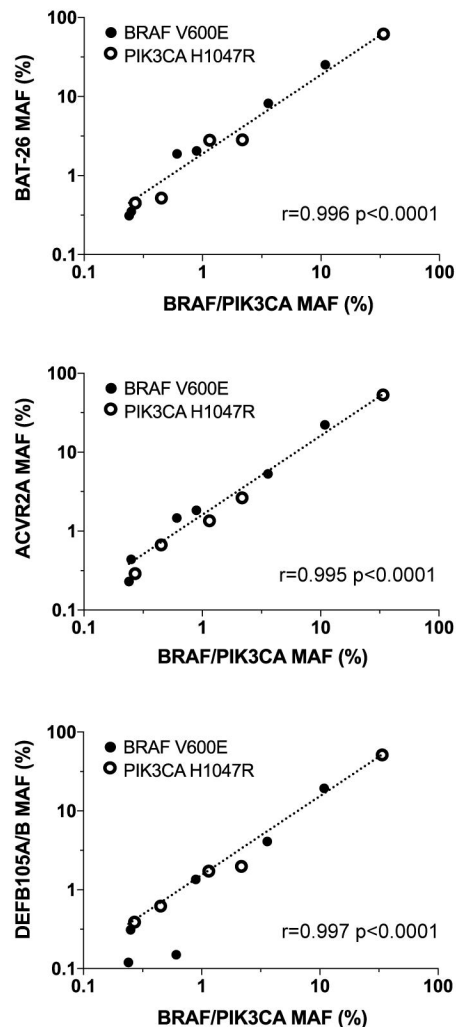


Fig. 3

A



B



○--- BRAF V600E or PIK3CA H1047R ▲--- ACVR2A
 ■--- BAT-26 ▼--- DEFB105A/B